ELSEVIER Science Press

Trans. Nonferrous Met. Soc. China 19(2009) s785−s789

Transactions of Nonferrous Metals Society of China

www.tnmsc.cn

# Crystal growth of tungsten during hydrogen reduction of tungsten oxide at high temperature

WU Xiang-wei(吴湘伟)[1, 2], LUO Jing-song(罗劲松)[2], LU Bi-zhi(陆必治)[2], XIE Chen-hui(谢晨辉)[2], PI Zhi-ming(皮志明)[2], HU Mao-zhong(胡茂中)[2], XU Tao(徐 涛)[2], WU Guo-gen(吴国根)[2], YU Zhi-ming(余志明)[1], YI Dan-qing(易丹青)[1]

1. School of Materials Science and Engineering, Central South University, Changsha 410083, China;
2. Zhuzhou Cemented Carbide Group Corp. Ltd., Zhuzhou 412000, China

Received 10 August 2009; accepted 15 September 2009

**Abstract:** Crystal growth of tungsten during hydrogen reduction of tungsten oxide ($WO_3$) to prepare coarse grain tungsten powder at high temperature (950 ℃) was studied. The phase composition and morphologies of products were investigated by means of XRD and SEM. The results show that the reduction sequence of hydrogen reduction of $WO_3$ is $WO_3 \rightarrow WO_{2.9} \rightarrow W_{18}O_{49} \rightarrow WO_2 \rightarrow W$. The step of $WO_2 \rightarrow W$ is the critical step which determines the grain size of tungsten powder. The partial pressure ($p_{H_2O}/p_{H_2}$) of $H_2O$ within powder layer shows strong effect on the nucleation and grain growth of tungsten. By increasing the $p_{H_2O}/p_{H_2}$ within powder layer, well-developed coarse grain tungsten powder with particle size above 15 μm is obtained. After carburizing, the powder can be used to produce ultra-coarse grain cemented carbide with grain size above 5 μm.

**Key words:** coarse grain tungsten powder; hydrogen reduction of tungsten oxide; crystal growth; partial pressure

## 1 Introduction

In these years, significantly incremental enhancements and specialized developments in the area of hardmetal continued shift towards ultra-fine and ultra-coarse grades[1]. Compared with conventional cemented carbide (middle grain or fine grain carbides), ultra-coarse grain cemented carbides(＞5 μm) demonstrate good fracture toughness and thermal fatigue resistance. Thus, they attract much attention from different departments in the area of industry. Currently, it is widely applied in many fields and found increasing usage in areas such as milling tools, punching dies, and boring drills[2−5]. Coarse grain W and WC powders are key materials for ultra-coarse grain cemented carbides producing. The industrially established method of preparing tungsten and carbide is the hydrogen reduction of tungsten oxide, tungstic acid or ammonium para tungstate at 900−1 200 ℃ or even higher temperature, initially to the metal powder followed by carburization. The average particle size of the powder obtained in this way is below 12 μm (Fsss)[6−7]. In order to obtain coarser powder, the normal method is reducing and carburizing treatment of tungsten oxide in the presence of alkali metal compounds at high temperature[8−11]. Thus, the obtained powder particle size can be above 50 μm (Fsss). But its defects and micro-strain are relatively more than those of the powder without addition of dopant. Some researches show that the crystalline perfection of tungsten carbide grain in the alloy can be impaired by tungsten starting material which undergoes the adulteration of alkali metal[12]. In this work, the crystal growth of tungsten during reducing tungsten trioxide at 950 ℃ under hydrogen and the effect of $H_2O$ partial pressure ($p_{H_2O}/p_{H_2}$) within powder layer on the nucleation and grain growth of tungsten were investigated.

## 2 Experimental

The commercially tungsten oxide ($WO_3$) with average Fsss size of 20 μm was used as starting material. Reduction experiments were carried out in a single-tube electrically heated push furnace with the size of 300 mm ×70 mm, and the length of 6 m, under counter-current flow of hydrogen. The highest temperature in the furnace tube was set at 950 ℃ and the flow rate of the incoming

**Corresponding author:** WU Xiang-wei; Tel: +86-13973125149; E-mail: xiangwei_wu@126.com

hydrogen was 10 $m^3$/h. The dew point of hydrogen was from −73 ℃ to −74 ℃. The boat was 250 mm long. The boatload of tungsten oxide was 4 kg, resulting in powder layer heights of 25 mm. The loaded boats were pushed to the furnace tube at the speed of one boat every 60 min. When the 20 loaded boats were pushed, holding for 60 min, and the reduction experiment was interrupted by importing pure argon (30 $m^3$/h) to replace the hydrogen atmosphere in furnace tube. Then the boats were pushed to the cooling zone under argon atmosphere. When being discharged after cooling, the reduction product was carefully sampled at the corresponding sites where the boats stayed in furnace tube when interrupting the reduction experiment. That is, the latest loaded boat pushed to the furnace tube was sampled as N1, and the first one sampled as N20. And in every boat, the powders in top layer, middle layer and bottom layer were sampled, respectively.

The phase analysis of the products was performed by XRD (X-ray powder diffraction) with Cu $K_\alpha$ radiation at 40 kV, 40 mA and 2.3 (°)/min. The morphological changes during reduction sequence were studied using SEM (scanning electronic microscope).

## 3 Results and discussion

### 3.1 Phase composition of products

The phase composition and the colour of the samples reduced from tungsten oxide by hydrogen at 950℃ are listed in Table 1. Since three boats of N1, N2 and N3 were still in the cooling zone near the feed end of the furnace tube when interrupting the reduction experiment, the tungsten oxides in these boats were not reduced by hydrogen. The colour of powders in boats from N4 to N9 changed greatly. The prezone of boat N4 was pushed to the heating zone, while the back zone was still in cooling zone. Three kinds of phases, $W_{18}O_{49}$, $WO_{2.9}$ and $WO_3$ were detected for the powders in the prezone of boat N4. Since the diffraction peaks of these phases seriously overlap, it was difficult to determine the content of each phase. $W_{18}O_{49}$ and $WO_2$ in boat N5 were detected. The content of $WO_2$ in this boat tended to increase from bottom layer to the top. Only $WO_2$ and W could be observed in boats from N6 to N9. The content of W in boat N6 was little. With the boats shifting forward, the

**Table 1** Phase composition and colour of samples

| Sample | | Phase composition | Colour |
|---|---|---|---|
| N1, N2, N3 | | $WO_3$ | Yellow |
| N 4 | Back zone* | $WO_3$ | Yellow, colour of bottom layer tends to blue |
| | Prezone* | $WO_3$, $WO_{2.9}$, $W_{18}O_{49}$ | Purple in middle-top layer, blue in bottom |
| N 5 | Top layer | 24.5%$W_{18}O_{49}$, 75.5%$WO_2$ | Brown in prezone, purple in back zone |
| | Middle layer | 38.4%$W_{18}O_{49}$, 61.6%$WO_2$ | |
| | Bottom layer | 69.2%$W_{18}O_{49}$, 30.8%$WO_2$ | |
| N 6 | Top layer | 96.7%$WO_2$, 3.3%W | Brown |
| | Middle layer | 97.3%$WO_2$, 2.7%W | |
| | Bottom layer | 98.5%$WO_2$, 1.5%W | |
| N 7 | Top layer | 77.0%$WO_2$, 33.0%W | Grey in prezone, brown in back zone |
| | Middle layer | 89.0%$WO_2$, 11.0%W | Brown |
| | Bottom layer | 92.0%$WO_2$, 8.0%W | Brown |
| N 8 | Top layer | 29.0%$WO_2$, 71.0%W | Grey-brown |
| | Middle layer | 46.0%$WO_2$, 54.0%W | Grey-brown |
| | Bottom layer | 75.6%$WO_2$, 24.4%W | Brown-grey |
| N 9 | Top layer | W | Grey |
| | Middle layer | 5.0%$WO_2$, 95.0%W | Grey |
| | Bottom layer | 17.0%$WO_2$, 83.0%W | Grey-brown |
| N 10−N 20 | | W | Grey |

Note: Prezone of boat turns towards discharged end of furnace, and back zone turns towards feed end of the furnace

content of W in boat increased. Among these boats (from N6 to N9), the content of W in each boat tended to increase from bottom layer to the top, and the powder in top layer of boat N9 was W. The materials in boats from N10 to N20 were all reduced to W. In all boat, W was in $\alpha$-W phase, and no $\beta$-W was detected.

### 3.2 SEM analysis of samples

All powder samples were identified by SEM. From the results shown by XRD analysis, no metal tungsten grain was observed for samples in boats from N1 to N5. And a small amount of W grain can be observed in $WO_2$ matrix for the sample of boat N6, which is shown in Fig.1(a). This indicated that the tungsten grain began to nucleate and grow in this reduction sequence. In the boat N7, the amount of W grain increased; the grain size also increased (Fig.1(b)); and the dimension was relatively uniform. While comparing the W grains observed among the samples of top, middle and bottom layer of boat N7, it was found that the amount of W grain in top layer was more than that of the middle or bottom layer, but the grain size was smaller. The amount of W grain among three powder layers of boat N8 was more than that of boat N7, but the difference of W grain size in two boats was little. In the boat N9, $WO_2$ in the top layer was all reduced to W, but the dimension of W grain was not uniform, and some small W grain appeared (Fig.1(c)). While in the middle and bottom layer of boat N9, some $WO_2$ phase could be observed (Fig.1(d)). No $WO_2$ phase was observed in boat N10. The morphology of W powder in top layer of boat N10 was similar to that of the top layer powder of boat N9. The morphologies of W powder in middle and bottom layer of boat N10 are shown in Figs.1(e) and (f), respectively. It can be seen

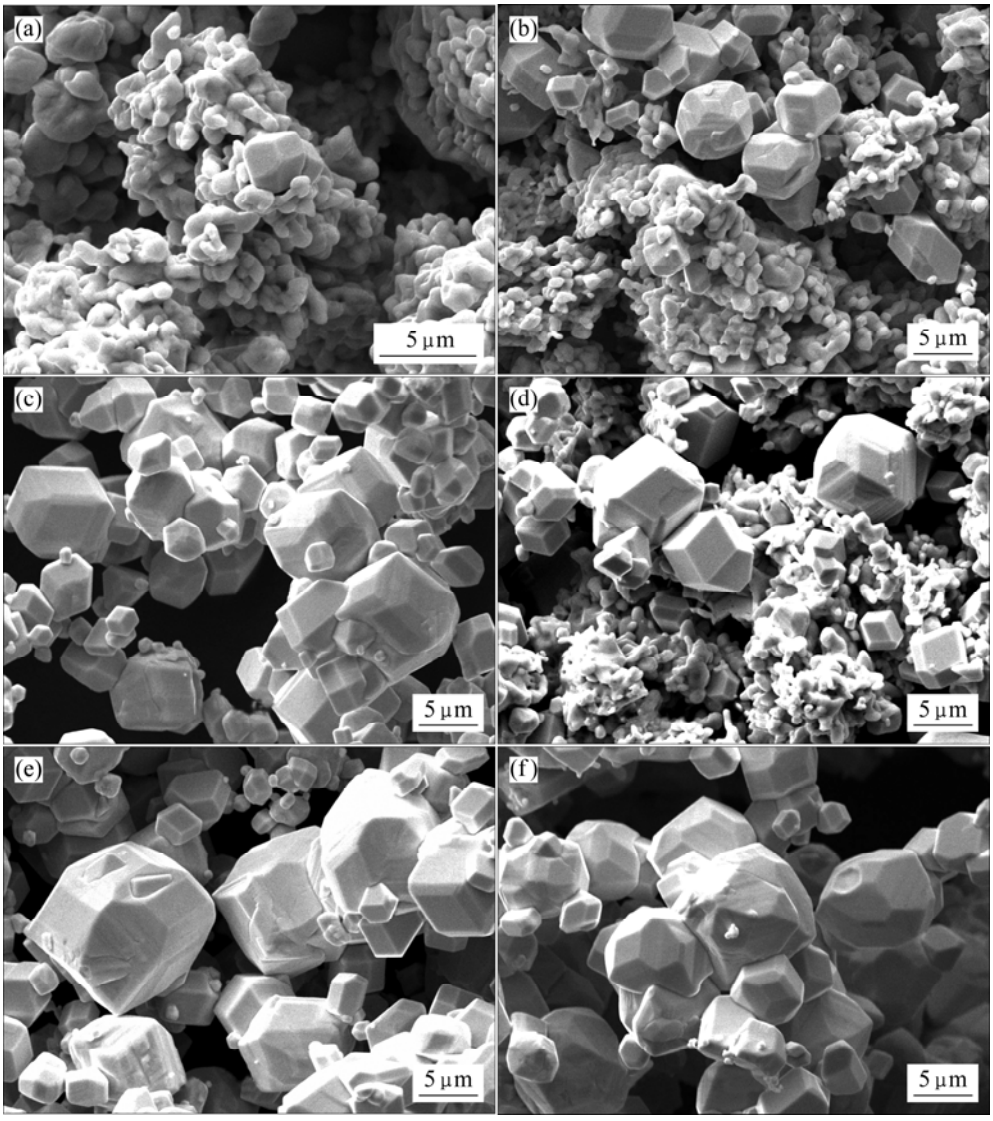


**Fig.1** Morphologies of powder in boat N6(a), N7(b), N9 top layer(c), N9 middle layer (d), N10 middle layer(e) and N10 bottom layer(f)

that some small W grains also appeared in middle and bottom layer of boat N10, and the size of part of W grains was even smaller than that of top layer.

The average Fsss sizes of W powder in boats from N10 to N20 are shown in Fig.2. It can be seen that Fsss size of W powder in the first boat (N20) pushed to the furnace tube was the smallest, and then increased in boats later pushed and tended to be stable from boat N17 to N10. In all boats, the Fsss sizes of W powder in bottom layer were larger than those in top or middle layer.

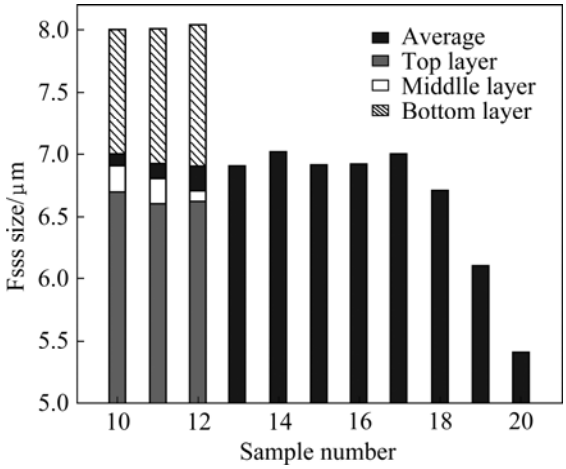


**Fig.2** Fsss size of W powder

### 3.3 Discussion

According to the results obtained from XRD and SEM analysis, tungsten oxide ($WO_3$) is reduced to metal tungsten at high temperature under hydrogen in the stepwise reduction sequence of $WO_3 \rightarrow WO_{2.9} \rightarrow W_{18}O_{49} \rightarrow WO_2 \rightarrow W$, which is consistent with result in Ref.[13]. Among these phase transitions, the first three transitions, $WO_3 \rightarrow WO_{2.9}$, $WO_{2.9} \rightarrow W_{18}O_{49}$, and $W_{18}O_{49} \rightarrow WO_2$, proceed very fast, and the overall reduction rate is limited mainly by the $WO_2 \rightarrow W$ transition. The nucleation and growth of W grain occur in the $WO_2 \rightarrow W$ transition. The technical conditions for $WO_2 \rightarrow W$ transition greatly affects the grain size, uniformity and crystalline of W powder.

Based on thermodynamics, the four reactions of $WO_3 \rightarrow WO_{2.9}$, $WO_{2.9} \rightarrow W_{18}O_{49}$, $W_{18}O_{49} \rightarrow WO_2$ and $WO_2 \rightarrow W$ are related to the $H_2O$ partial pressure, $p_{H_2O}/p_{H_2}$, at a fixed temperature[13−14]. The relationship of the equilibrium $\lg(p_{H_2O}/p_{H_2})$ of the four reactions with $1/T$ is shown in Fig.3. At a fixed temperature, the equilibrium $p_{H_2O}/p_{H_2}$ of $WO_2 \rightarrow W$ is the lowest. In this experiment, counter-current flow of hydrogen with a dew point form −73 ℃ to −74 ℃ was used. The $H_2O$ in hydrogen mainly came from the reaction of tungsten oxide with hydrogen. After the loaded boat was moved to site of boat N10 and held for 1 h, all materials in the boat were

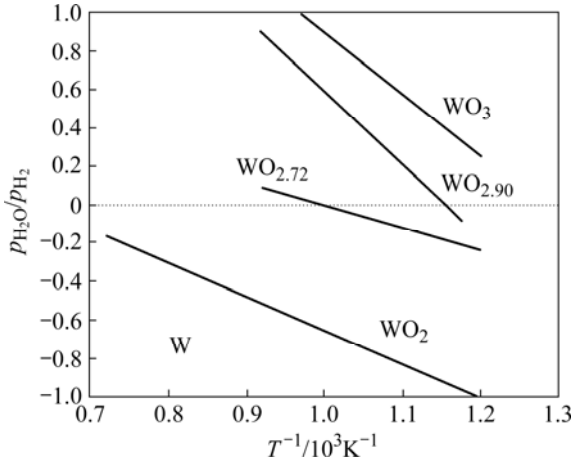


**Fig.3** Equilibrium curves of different tungsten oxides and tungsten

reduced to metal tungsten. So, the powders in boats from N11 to N20 no more generated $H_2O$. The $H_2O$ generated by the reduction of tungsten oxide in boats from N10 to N4 diffused into hydrogen atmosphere and flowed to the feed end of the furnace tube with hydrogen. If the reduction of tungsten oxide to tungsten is in uniform speed, the $\lg(p_{H_2O}/p_{H_2})$ of the hydrogen passing through boats from N10 to N6 can be calculated, respectively, to be −1.70, −1.40, −1.22, −1.10 and −1.00, which are much lower than the equilibrium $\lg(p_{H_2O}/p_{H_2})$ of the reaction $WO_2 \rightarrow W$ at 950 ℃.

On the other hand, $WO_2$ and $H_2O$ can form volatile tungsten oxide-hydroxide during reduction, and then the tungsten grain grows through CVT (chemical vapour transport) reaction [13, 15]:

$$WO_2(OH)_2(g) + 3H_2 \rightleftharpoons W(s) + 4H_2O(g) \quad (1)$$

When the $p_{H_2O}/p_{H_2}$ in hydrogen atmosphere is high, the nucleation is limited; tungsten grain grows; and coarse-grain tungsten powder can be obtained. On the contrary, fine powder appears. In order to obtain coarse-grain tungsten powder, the transition of $WO_2 \rightarrow W$ must proceed under relatively high $p_{H_2O}/p_{H_2}$ in hydrogen atmosphere throughout.

By controlling the $p_{H_2O}/p_{H_2}$ in hydrogen atmosphere at 0.4−0.5, uniformly and well-developed coarse-grain tungsten powder with Fsss size of 21 μm was obtained at 1 000 ℃ (Fig.4(a)). The coarse-grain tungsten powder was blended with C and carburized at temperature above 2 000 ℃, then coarse-grain WC powder was obtained. The WC powders were wet ball-milled with 17% (mass fraction) Co powders for 16 h at a ratio of balls to materials of 3:1. After being dried and compacted, the compacted powders were consolidated by liquid phase sintering at 1 450 ℃ for 1 h. The WC grain size in cemented carbide was above 5 μm (Fig.4(a)).

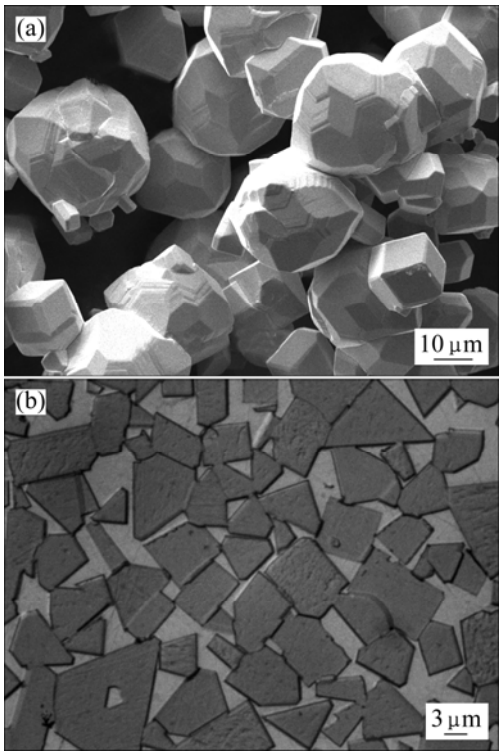


**Fig.4** Morphologies of coarse-grain tungsten (a) and WC-Co alloy (b)

## 4 Conclusions

1) At high temperature, yellow tungsten oxide ($WO_3$) is reduced to metal tungsten under hydrogen in the stepwise reduction sequence of $WO_3 \rightarrow WO_{2.9} \rightarrow W_{18}O_{49} \rightarrow WO_2 \rightarrow W$. The overall reduction rate is limited mainly by the $WO_2 \rightarrow W$ transition. The nucleation and growth of W grain occur in the $WO_2 \rightarrow W$ transition.

2)The technical conditions of $WO_2 \rightarrow W$ transition greatly affect the grain size, uniformity and crystalline of W powder.

3) In order to obtain coarse-grain tungsten powder, the transition of $WO_2 \rightarrow W$ must proceed under relatively high $p_{H_2O}/p_{H_2}$ in hydrogen atmosphere throughout.

## References

[1] NORTH B. Global trends in hard materials [C]// KNERINGER G, RÖDHAMMER P, WILDNER H. Proceedings of 16th International Plansee Seminar. Reutte, Austria: Plansee Nolding AG, 2005: 1−8.

[2] ZHANG Jun-xi. Effect of reduction and carburization temperature of tungsten powder on WC-phase substructure and mechanical properties of WC-Co cemented carbide [J]. Int J Refract Met Hard Mater, 1988, 7(4): 224−228.

[3] JORG BREDTHAUER B, BENNO GRIES W, BERNHARD SZESNY L. Ultra-coarse, monocrystalline tungsten carbide and a process for the preparation thereof, and hardmetal produced therefrom: US 20020078794A1[P]. 2002−06−27.

[4] KONYASHIN I, SCHAFER F, COOPER R, RIES B, MAJOR J, WEIRICH T. Novel ultra-coarse hardmetal grades with reinforced binder for mining and construction [J]. Int J Refract Met Hard Mater, 2005, 23(4/6): 225−232.

[5] KIM Y P, JJUNG S W, KANG S J, KIM B K. Enhanced densification of liquid-phase-sintered WC-Co by use of coarse WC powder: Experimental support for the pore-filling theory [J]. Journal of the American Ceramic Society, 2005, 88(8): 2106−2109.

[6] TAO Zheng-ji. Study of carburization of coarse tungsten powder [J]. Int J Refract Met Hard Mater, 1987, 6(4): 221−225.

[7] LASSNER E. Influence of carburization temperature on tungsten carbide properties [J]. Int J Refract Met Hard Mater, 1989, 8(3): 185−188.

[8] ZHENG Feng. Effect of some metal elements on particle size of tungsten powder [J]. Cemented Carbide, 1995, 12(3): 143−145. (in Chinese)

[9] SUN Bao-qi, CHEN Yi-ming. Investigation on preparation of coarse crystal W powder through Li-activated $H_2$ [J]. Rare Metal and Cemented Carbide, 1999(1): 1−6. (in Chinese)

[10] FU Lian-ying. Influence of sodium content in blue tungsten oxide on particle size of W and WC powder [J]. Cemented Carbide, 1995, 12(4): 216−222. (in Chinese)

[11] HAUBNER R, SCHUBERT W D，LUX B. Influence of aluminum on the reduction of tungsten oxide to tungsten powder [J]. Int J Refract Met Hard Mater, 1987, 6(3): 161−167.

[12] ZHANG Li, WANG Yuan-jie, YU Xian-wang, WANG Zhen-bo. Effect of particle size and morphology of tungsten carbide powder on grain size, grain morphology and properties of cemented carbide [J]. China Tungsten Industry, 2008, 23(4): 223−26. (in Chinese)

[13] SCHUBERT W D. Kinetics of the hydrogen reduction of tungsten oxides [J]. Int J Refract Met Hard Mater, 1990, 9(3): 178−191.

[14] WANG Guo-dong. Theory of cemented carbide production [M]. Beijing: Metallurgical Industry Press, 1992: 10−20. (in Chinese)

[15] SCHUBERT W D. Production and characterization of hydrogen-reduced submicron tungsten powders-part1: State of the art in research, production and characterization of raw materials and tungsten powders [J]. Int J Refract Met Hard Mater, 1991, 10(3): 133−141.

**(Edited by YANG Hua)**